Molecular Biology of the Cell
Vol. 9, 2667–2680, September 1998

The Dynamics of Golgi Protein Traffic Visualized in Living Yeast Cells

Steven Wooding and Hugh R.B. Pelham*

MRC Laboratory of Molecular Biology, Cambridge CB2 2QH, United Kingdom

Submitted May 17, 1998; Accepted July 9, 1998
Monitoring Editor: Randy W. Schekman

We describe for the first time the visualization of Golgi membranes in living yeast cells, using green fluorescent protein (GFP) chimeras. Late and early Golgi markers are present in distinct sets of scattered, moving cisternae. The immediate effects of temperature-sensitive mutations on the distribution of these markers give clues to the transport processes occurring. We show that the late Golgi marker GFP-Sft2p and the glycosyltransferases, Anp1p and Mnn1p, disperse into vesicle-like structures within minutes of a temperature shift in *sec18*, *sft1*, and *sed5* cells, but not in *sec14* cells. This is consistent with retrograde vesicular traffic, mediated by the vesicle SNARE Sft1p, to early cisternae containing the target SNARE Sed5p. Strikingly, Sed5p itself moves rapidly to the endoplasmic reticulum (ER) in *sec12* cells, implying that it cycles through the ER. Electron microscopy shows that Golgi membranes vesiculate in *sec18* cells within 10 min of a temperature shift. These results emphasize the dynamic nature of Golgi cisternae and satisfy the kinetic requirements of a cisternal maturation model in which all resident proteins must undergo retrograde vesicular transport, either within the Golgi complex or from there to the ER, as anterograde cargo advances.

INTRODUCTION

The Golgi apparatus occupies a central position in the secretory pathway of eukaryotic cells. It is the site at which membrane proteins and lipids are modified and sorted, and it acts as a filter between the phospholipid-rich endoplasmic reticulum (ER) and the sphingolipid- and sterol-rich plasma membrane. Proteins are transferred from the ER to early or cis-Golgi compartments in a process that involves the formation and fusion of small transport vesicles (Palade, 1975; Rothman, 1994; Schekman and Orci, 1996). They subsequently leave from a late-Golgi compartment, known in animal cells as the trans-Golgi network, and move to the plasma membrane or to endosomes, again in vesicles or larger membrane-bound carriers. However, the mechanism by which proteins are transferred from early- to late-Golgi compartments has proven more controversial (Farquhar, 1985; Schekman and Mellman, 1997; Pelham, 1998).

A popular model assumes that Golgi cisternae have a stable existence and that transport between them occurs by means of vesicular carriers, with resident proteins being returned to the ER or to earlier Golgi compartments by a separate set of retrograde vesicles (Farquhar, 1985; Rothman, 1994). An alternative view, derived from the original concept of cisternal maturation, is that cisternae move progressively through the Golgi stack, with vesicular traffic being used only to retrieve resident proteins from more mature cisternae and deliver them to newly formed ones (Schnepf, 1993; Pelham, 1998). Alternative models have also been proposed that invoke the transient or permanent connection of cisternae by tubules, thus eliminating the need for vesicular traffic altogether (Mironov *et al.*, 1997). Distinguishing between these models is important because they suggest different molecular mechanisms for the sorting of membrane components. However, it is not easy because the models can be varied to fit many observations, and information on the precise pathways followed by proteins within and around the Golgi complex is limited.

The realization that membrane fusion events in the secretory pathway are mediated by SNARE proteins has allowed a new approach to this problem. SNAREs are integral membrane proteins found in vesicles (des-

* Corresponding author.

ignated v-SNAREs) and on organellar membranes (designated target or t-SNAREs) that combine to form specific coiled-coil structures. These structures can be disrupted by the action of other proteins named NSF and SNAP, or Sec18p and Sec17p in yeast, which are themselves required for membrane fusion (reviewed by Rothman, 1994). Formation of SNARE complexes that bridge the two membranes is required for fusion to occur (Nichols *et al.*, 1997). Hence, examination of the full complement of SNAREs in yeast, where the genome sequence is complete, can place limits on the number and nature of transport steps that involve fusion. Temperature-sensitive SNARE mutants can be used to block these steps.

A common feature of these fusion events is the requirement for a member of the syntaxin family of t-SNAREs. In yeast, at least two syntaxins are present in the Golgi complex: Sed5p, which defines an early compartment, and Tlg2p, which is found in a distinct late compartment (Hardwick and Pelham, 1992; Holthuis *et al.*, 1998). Another syntaxin Tlg1p is in a compartment to which late Golgi markers such as Kex2p have access, although whether this should be considered part of the Golgi complex or endosomal is debatable (Holthuis *et al.*, 1998). In addition, at least three putative-vesicle SNAREs have been identified in the Golgi, namely Sft1p, Gos1p, and Vti1p (Banfield *et al.*, 1995; McNew *et al.*, 1997; Fischer von Mollard *et al.*, 1997; Lupashin *et al.*, 1997). Of these, Vti1p binds to Tlg2p and Tlg1p and could, in principle, mediate forward vesicular traffic to a late-Golgi compartment (Holthuis *et al.*, 1998). However, since neither Tlg1p nor Tlg2p is required for secretion, such a step may not be necessary for proteins to progress through the Golgi complex. On the other hand, Sft1p is essential for intra-Golgi transport, and Sft1p, Gos1p, and Vti1p all bind to Sed5p. We have argued that these results are most consistent with a specific version of the cisternal maturation model in which vesicular traffic back to the Sed5p-containing compartment is an essential element (Holthuis *et al.*, 1998; Pelham, 1998). This model also requires that Sed5p itself is removed from cisternae as they mature, presumably in vesicles.

Tests of such models require analysis of the dynamics of protein movement within the Golgi complex, and this has been hindered in yeast by the poorly defined and scattered nature of the organelle. In this paper we describe visualization of yeast Golgi membranes in living cells, using green fluorescent protein (GFP)-tagged proteins. As markers we have chosen Sed5p and Sft2p. Sft2p is a membrane protein apparently located in the late Golgi, which interacts genetically with the early-Golgi "target" SNARE, Sed5p (Banfield *et al.*, 1995). We show that GFP-Sft2p labels Golgi membranes, that it can enter smaller, presumably vesicular structures, and that the fusion of these requires Sec18p, Sft1p, and Sed5p. The Golgi mannosyltransferases, Anp1p and Mnn1p, also disperse under these conditions, suggesting retrograde vesicular transport of these proteins within the Golgi complex. Strikingly, we find that Sed5p itself is not a permanent resident of the Golgi, but recycles through the ER. The kinetics of these events are consistent with a key assumption of the cisternal maturation model, namely that all resident Golgi proteins can be removed from cisternae within the time taken for secretory proteins to pass through the Golgi complex.

MATERIALS AND METHODS

Yeast Strains

The *SEC*$^+$ strain used was SEY6210 (*MATα ura3–52 leu2–3, -112 his3-Δ200 trp1-Δ901 lys2–801 suc2-Δ9*). Mutant strains constructed from this were DB51 (*MATα ura3–52 leu2–3, -112 his3-Δ200 trp1-Δ901 lys2–801 suc2-Δ9 sed5–1*), DB115 (*MATα ura3–52 sft1::LEU2 leu2–3, -112 his3-Δ200 trp1-Δ901 suc2-Δ9 lys2–801* containing pSFT115 [*CEN6 HIS3 sft1–15*]), and SW14B3 (*sec14–3 ura3–52 leu2–3, -112 his3-Δ200, trp1-Δ901*). Other sec mutants, RSY271 (*MATα sec18–1 ura3–52 his4–619*) and RSY263 (*MATα sec12–4 ura3–52*), were from C. Kaiser. Plasmids expressing GFP chimeras were inserted into these strains by simple integration (allowing multiple tandem insertions) at *URA3*, and transformants were screened for optimal GFP fluorescence. The SEY6210 derivative expressing both chimeras had the GFP-Sed5p construct inserted at *URA3* and the GFP-Sft2p construct at *LEU2*.

Plasmids

GFP chimeras were expressed from derivatives of p406TXH, a *URA3* integration vector derived from pRS406 (Sikorski and Hieter, 1989) by insertion of the *TPI* promoter between the *Xho*I and *Hind*III sites of the polylinker. The coding sequence for the mut2 version of GFP, described by Cormack *et al.* (1996), or the W7 mutant of Heim and Tsien (1996) was cloned by PCR between the *Hin*dIII and *Eco*RI sites of the polylinker. The *SED5*- and *SFT2*-coding regions were then fused to GFP at the *Eco*RI site. The resultant amino acid sequence at the junction was YKSNSMNI for GFP-Sed5p and YKSNSMSE for GFP-Sft2p. For the double-label GFP experiments, the *TPI* promoter and fusion gene were transferred into the *LEU2* integration vector pRS405 (Sikorski and Hieter, 1989). N-terminally triple myc-tagged Sft1p was expressed from the *TPI* promoter in p405TSF13M (a pRS405 derivative), integrated at *LEU2*. A *TRP1 CEN* plasmid expressing, from its own promoter, Mnn1p tagged at the C terminus with three copies of the influenza hemagglutinin (HA) epitope was kindly provided by Sean Munro. N-terminally triple HA-tagged Sed5p was expressed from the TPI promoter, integrated at *URA3*.

Immunodetection

Cells were prepared for immunofluorescence using a variation of the method of Kilmartin and Adams (1984). Log phase cells were fixed by adding 2.5 ml of fresh 10% paraformaldehyde to 7.5 ml of yeast culture and pelleted by centrifugation. They were resuspended in 3.2 ml of 0.1 M KPO_4 (pH 7.5), 1.8 ml of paraformaldehyde solution were added, and fixation was continued for an additional 15 min. Cells were then washed four times in KPO_4 and resuspended in 1 ml of SPP (1.2 M sorbitol, 0.1 M KPO_4, pH 7.5) containing 100 mM DTT, after which a few flakes of lyophilized oxalyticase (Enzogenetics, Corvallis, OR) were added, and incubation was continued at 30°C. Cell wall digestion was monitored by diluting samples into water, and, when complete, the spheroplasts were harvested by centrifugation and resuspended in 50 mM NH_4Cl

in SPP to quench free aldehyde groups, and then in SPP before being transferred to polylysine-coated slides. The slides were immersed in methanol for 6 min and acetone for 30 s, both at −20°C, and then air dried.

Antibody staining was performed as described by Lewis and Pelham (1996), as was the preparation of whole-cell extracts, fractionation into medium-speed (p13) and high-speed (p100) membrane pellets, and immunblotting. Rabbit anti-Anp1p (Jungmann and Munro, 1998) was kindly provided by Joern Jungmann. Yeast binding protein (BiP) was detected with mAb 2E7 (Napier *et al.*, 1992), Sed5p with rabbit antiserum (Holthuis *et al.*, 1998), and GFP (on blots) with a mixture of mAbs 7.1 and 13.1 (Boehringer Mannheim, Germany). The influenza HA and myc epitopes were detected with rabbit polyclonal IgG (Santa Cruz Biotechnology, Santa Cruz, CA).

Preparation of Cells for Live Imaging

An observation chamber was constructed consisting of a 5-mm-thick aluminum alloy block the size of a standard glass microscope slide, through the center of which was bored an 18-mm diameter hole, reamed out to 19.5 mm to a depth of 0.5 mm. A 19-mm coverslip was sealed in place in the hole with Superglue to form the base of the chamber. The chamber was overfilled with ~1 ml of molten agar containing minus uracil growth medium and covered with a glass microscope slide until the agar had set. The slide was supported on coverslips to ensure that the resulting agar pad extended slightly above the metal slide. Excess agar was removed from the metal, and then 2–3 μl of yeast cells were spread on the agar pad and covered with a 22-mm coverslip, which was fixed in position with nail varnish. For experiments in which the cells were to be heated, the metal chamber was modified by the addition of two heat sink mounting resistors and monitor thermistors. A thermocouple was mounted in the agar immediately below the yeast cells to allow accurate recording of their temperature. Heating was controlled by a TC-334 Dual Heater Controller from Warner Instrument (Hamden, CT); however, in some experiments, heating was achieved by means of a hot-air fan directed at the slide.

Image Collection and Processing

Images were collected using an MRC600 confocal system (Bio-Rad, Richmond, CA) on a Diaphot-2 microscope (Nikon, Melville, NY), fitted with a 15 mW argon/krypton mixed-gas laser (Ion Laser Technologies). For double- label analysis of fixed samples, multiple images at evenly spaced focal planes through the cells were collected, using separate excitation for each fluorophore. For live cells, a single scan was used for each image, to minimize blurring due to movement. The 488-nm laser line was used for GFP excitation, with the intensity attenuated to 3%. Photobleaching was achieved by one slow scan with the laser intensity set at 100%.

Images were processed on Macintosh computers using the public domain NIH Image program (written by Wayne Rasband at the U.S. National Institutes of Health and available by anonymous ftp from zippy.nimh.nih.gov) to make maximum brightness projections and to allow background subtraction and adjustment of brightness. Gaussian blurring was used to reduce high-frequency noise. For each experiment involving a time course with live cells, images were taken without alteration of the microscope settings and processed in parallel, to ensure that they were comparable. The only exception is shown in Figure 5A, in which the later images were adjusted in brightness to compensate for progressive bleaching of the GFP. This was achieved simply by multiplying pixel values by a constant, after background subtraction, to ensure that the relative intensity distribution in each image (its apparent punctateness) was unaffected.

To obtain the histograms of pixel intensity, five to eight cells (not necessarily those shown in the figures, but from the same primary images) were outlined in NIH Image, and histogram values for the enclosed areas were obtained. The primary images had first been Gaussian blurred, and the histogram values were further smoothed by taking a seven-point running average. Each graph shows data from the same group of cells under the various conditions. Note that variations in the precision with which the cells were outlined could affect the low-pixel-intensity region of the graphs but cannot account for changes in the number of brighter pixels, which were well within the enclosed area. Note also that pixel values are not a measure of the absolute brightness of the cells, since they depend on the microscope settings used for each time course experiment.

Double-label GFP images (Figure 1C) were taken using excitation and emission filters designed for fluorescein, except that a lucifer yellow excitation filter was used for the W7 variant. Images were recorded on a cooled charge coupled device-based DeltaVision microscope system supplied by Applied Precision (Issaquah, WA) and deconvoluted using Delta Vision image analysis software.

Electron Microscopy

Cells were permanganate fixed, sectioned, and stained, and small vesicles were analyzed as described previously (Kaiser and Schekman, 1990; Lewis and Pelham, 1996). Unselected areas of the sections were photographed, and Golgi membranes, defined as darkly staining profiles that were neither juxtaposed to the cell wall, nor obviously connected to the peripheral ER or nuclear envelope, were measured in 60 cell sections.

RESULTS

Labeling of Sed5p and Sft2p with GFP

In initial experiments the lumenal domains of a variety of Golgi proteins were tagged with GFP and expressed in yeast, but in no case did we obtain a satisfactory fluorescent signal corresponding to Golgi membranes, possibly due to inefficient folding of GFP in the yeast ER lumen or to poor retention in the Golgi complex. However, successful labeling was obtained when GFP was fused to the first residues of Sed5p and Sft2p, Golgi membrane proteins whose N termini are predicted to be cytoplasmic. These chimeric proteins were therefore characterized in more detail.

Sed5p is a t-SNARE present in early Golgi cisternae and is essential for growth (Hardwick and Pelham, 1992). We found that the GFP-tagged version, expressed from a chromosomally integrated construct, could maintain growth of cells lacking the endogenous protein. Immunoblotting showed that the chimera was expressed at levels comparable to those of Sed5p itself and was largely intact (Figure 1B). Fluorescence microscopy revealed a punctate pattern similar to the immunofluorescence pattern of Sed5p. When the cells were fixed and stained with antibodies to the early Golgi marker Anp1p, there was extensive, although not perfect, overlap of the patterns (Figure 1A). Similar results were obtained previously when Anp1p and myc-tagged Sed5p were compared (Jungmann and Munro, 1998). Thus, the GFP-tagged protein evidently retains its normal localization and function. Staining with an antibody to luminal ER proteins confirmed that the ER remained intact in the cells and was clearly distinguishable from the membranes con-

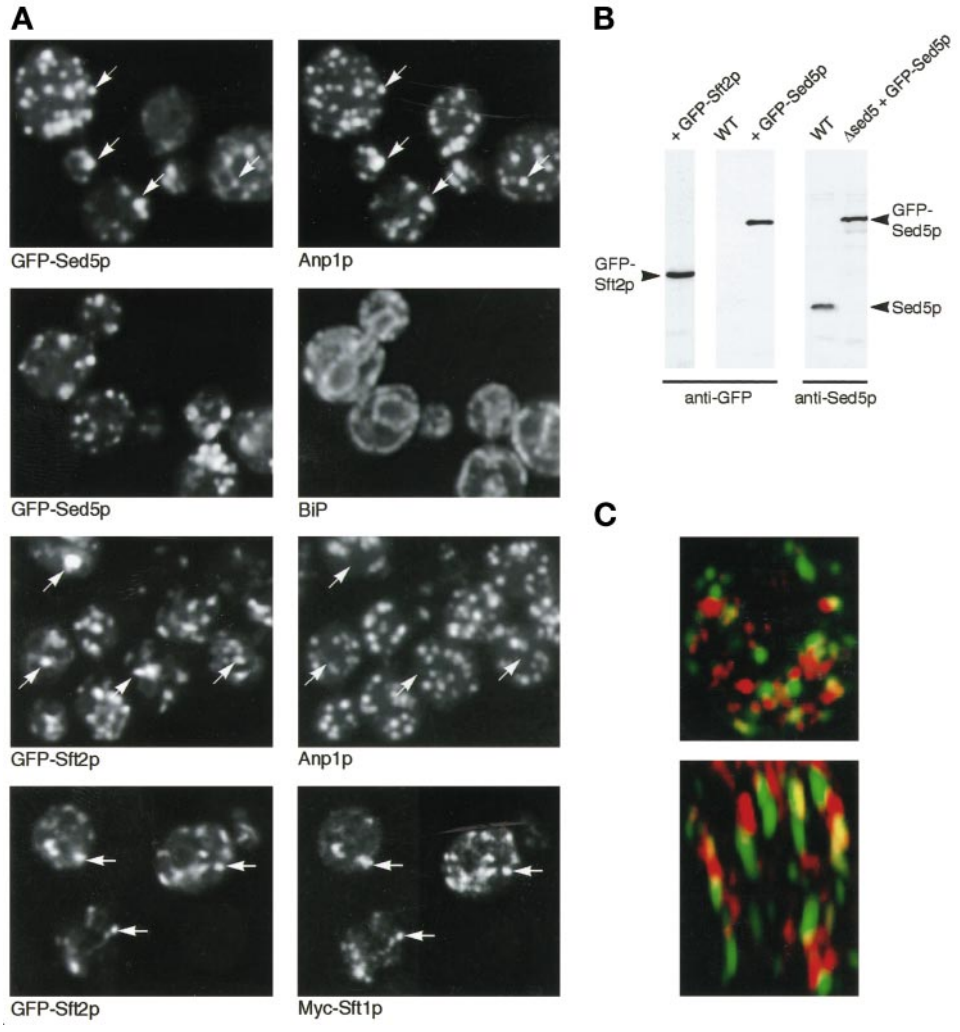

Figure 1. Localization of GFP-Sed5p and GFP-Sft2p. (A) Comparison of GFP fluorescence with immunofluorescent staining of marker proteins. Each pair of panels shows the same cells with the indicated markers; arrows indicate similarities and differences. The comparisons with Anp1p are projections of multiple confocal images spanning the entire thickness of the cells; others are single confocal planes. (B) Immunoblots of whole-cell extracts from strains expressing the indicated chimeras, probed with anti-GFP or anti-Sed5p. (C) Double label with two different GFP variants. A reconstruction of a single living cell is shown, viewed from above (top) and from the side (bottom). Streaking in the side view is due to lower optical resolution in the vertical dimension. Red corresponds to GFP-Sed5p; green represents an Sft2p chimera with the W7 variant of GFP.

taining GFP-Sed5p (Figure 1*A*). As observed with Sed5p itself, overexpression of GFP-Sed5p slowed growth, the effect being greater when the expression level was higher. For subsequent experiments, we selected transformants expressing 1–2 times as much GFP-Sed5p as endogenous protein, whose growth rate was within 20% of that of the parental strains.

Sft2p is predicted to have four transmembrane domains. Deletion of *SFT2* is not normally lethal, but we have recently isolated mutants that require Sft2p for growth (Conchon and Pelham, unpublished observations). GFP-Sft2p was tested in one such mutant, and we found that it retained the growth-promoting function of Sft2p. Immunoblotting with antibodies against GFP showed a single prominent band (Figure 1B), but since we have so far been unable to obtain antibodies that recognize the endogenous protein, we were unable to compare the expression level of the fusion protein with that of Sft2p itself.

We have previously shown that N-terminally myc-tagged Sft2p colocalizes with Sft1p in late Golgi cisternae largely distinct from the early ones marked by Sed5p (Banfield *et al.*, 1995). GFP-Sft2p behaved similarly, colocalizing with a myc-tagged version of Sft1p but showing little overlap with Anp1p (Figure 1A). In cells expressing high levels of GFP-Sft2p we also observed some labeling of vacuolar membranes, suggesting that retention of the protein in the Golgi was imperfect; for subsequent experiments we selected transformants that gave primarily a punctate pattern.

To compare directly the distributions of GFP-Sed5p and GFP-Sft2p in vivo, we constructed a strain expressing both chimeras, Sft2p being linked to the W7 mutant form of GFP, which has altered spectral characteristics (Heim and Tsien, 1996). Suitable excitation and emission filters allowed the two GFPs to be imaged separately, and a three-dimensional reconstruction of a live cell was prepared. As shown in Figure 1C, this revealed little overlap between the two markers, which were distributed in discrete punctate structures scattered throughout the cell. We conclude that the proteins are largely in separate compartments,

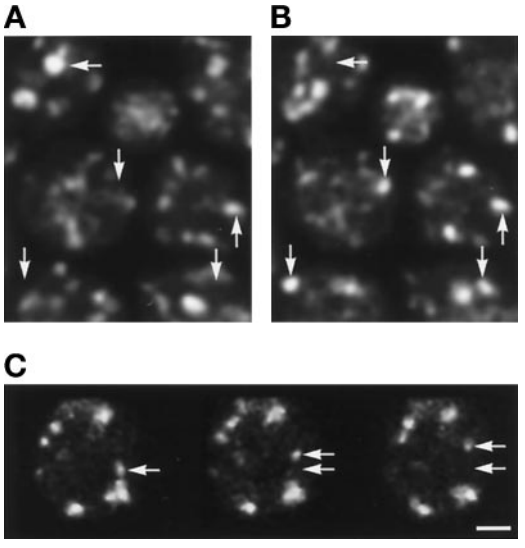

Figure 2. Movement of Golgi elements. Panel A shows two images of live cells expressing GFP-Sft2p, taken 1-min apart. Four optical sections spaced 1.5 μm apart (spanning the cell thickness) have been projected into a single image to minimize changes caused merely by objects shifting out of one focal plane. Arrows indicate differences in some, but not all, structures. Panel B shows single optical sections of a cell expressing GFP-Sed5p, taken 1.15 s apart. Arrows indicate the original and new position of one structure in this plane, which appears to undergo rapid movement. Bar, 1 μm.

which are not closely associated with each other in vivo. Unfortunately, rapid bleaching of the W7 GFP made more extensive double-label observations impractical.

Observation of the Yeast Golgi

We observed Golgi membranes in living yeast cells using confocal microscopy of cells growing on agar, an arrangement that maintained the growth and viability of the cells throughout the observations (see MATERIALS AND METHODS). The punctate appearance of the Golgi visualized with either GFP-Sed5p or GFP-Sft2p was similar to that observed with fixed cells. Time-lapse studies showed that with either marker the fluorescent structures moved irregularly within growing cells. Movement appeared undirected but was sufficiently rapid that it was very difficult to follow individual structures for prolonged periods. Some appeared to move at rates of up to 0.3 μm s^{-1} (Figure 2B), and substantial changes could be observed within a minute (Figure 2A). Treatment of cells with sodium fluoride, azide, and 2-deoxyglucose to reduce ATP levels greatly reduced the movement. Apparent fusion and scission events were sometimes observed, together with the appearance and disappearance of individual structures, but the uncertainties imposed by the limits of optical resolution and the rapid movement of the Golgi structures made interpretation of such events difficult. In particular, we were unable to determine whether individual Golgi cisternae in growing cells have an essentially permanent existence, the changes being due only to movement, or whether they have a limited life, as predicted by a cisternal maturation model. Instead, we adopted a genetic approach to the analysis of Golgi traffic.

Entry of GFP-Sft2p into Presumptive Retrograde Transport Vesicles

The resolution and sensitivity of light microscopy does not allow individual transport vesicles to be readily observed in yeast cells. We therefore used temperature-sensitive mutants that are predicted to block various stages of vesicular traffic to follow the movement of GFP-Sft2p. These experiments made use of a microscope stage that could be heated by up to 10°C per minute, allowing the immediate effects of the block to be observed. A control experiment using a *SEC*$^+$ strain showed that heating from 20°C to 37°C had little effect on the GFP-Sft2p pattern (Figure 3), although the fluorescent spots appeared slightly dimmer at the higher temperature.

The experiment was then repeated using the well-characterized *sec18–1* mutant, which rapidly inactivates the yeast homologue of NSF at elevated temperature and thus blocks most membrane fusion events (Graham and Emr, 1991). In this case, there was a dramatic change at the nonpermissive temperature (Figure 3). The bright spots of GFP-Sft2p disappeared and were replaced by a more even or much more finely punctate fluorescence that filled most of the cell, except for dark patches corresponding to nuclei and vacuoles. The change was confirmed by plotting histograms of pixel intensities over a region containing six cells. Initially, the intensities were spread quite widely, reflecting the presence of bright patches and a dim background, but at high temperature the profile for the same cells showed a tighter distribution, with the majority of the pixels having a moderate intensity (Figure 3). This pattern is consistent with the entry of GFP-Sft2p into a large number of small structures, presumably vesicles, that are not fully resolved by the microscope. The change occurred rapidly as the temperature was raised and was complete within 10 min. It was reversed upon cooling, consistent with a resumption of vesicle fusion (Figure 3). We observed some diffuse background fluorescence even in wild-type cells; this fluorescence was higher than the autofluorescence seen in cells not expressing GFP. We observed similar diffuse background fluorescence in *sec18* cells at low temperature. This may represent a steady-state level of vesicles; electron microscopic observations show that several hundred transport vesi-

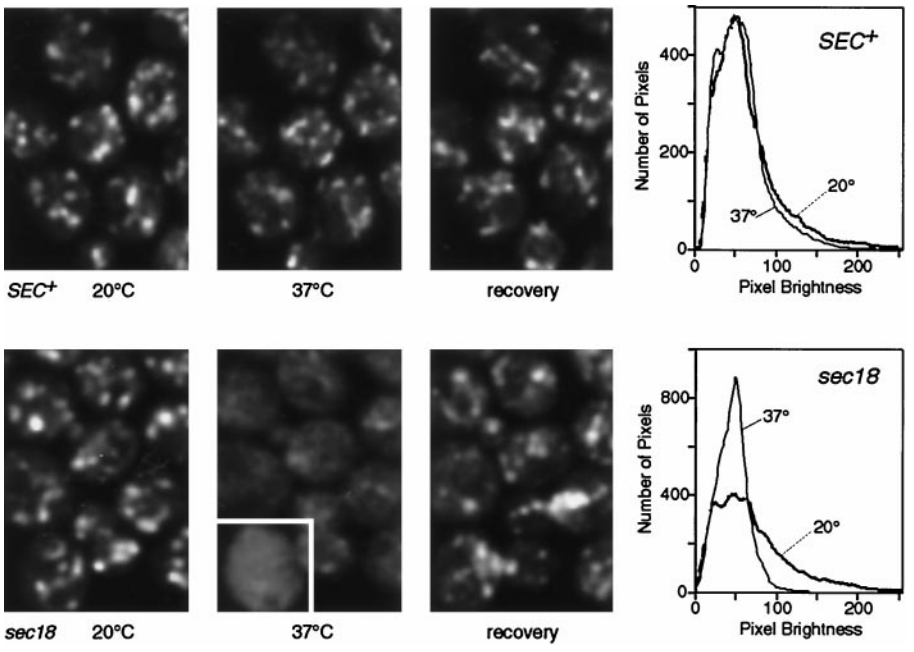

Figure 3. Dispersal of GFP-Sft2p in a *sec18* mutant. The upper panels show a control with *SEC*$^+$ cells, the same group of cells being imaged at 20°C, 10 min after initiation of warming to 37°C (i.e., after about 8 min at this temperature), and after re-equilibration to 20°C (20 min after heating stopped). The lower panels show the equivalent experiment with *sec18* cells. In the 37°C panel one cell (outlined in white) is printed with the brightness increased, to show more clearly the lack of punctate staining under these conditions. Images are projections of four optical sections. The graphs show smoothed profiles of the distribution of pixel brightness in groups of five to eight cells imaged successively at low and high temperature, obtained as described in MATERIALS AND METHODS. Note the loss of the brighter pixels at 37°C in the *sec18* cells.

cles are typically present in a wild-type cell, although their origin is not known (Kaiser and Schekman, 1990).

Fusion of Sft2p-containing Structures Requires Sft1p and Sed5p

If the structures that Sft2p enters are vesicles destined for early- Golgi compartments, their fusion should depend on Sed5p. To test this, the fate of GFP-Sft2p was examined in the temperature-sensitive allele *sed5–1*. A potential complication is that *SFT2* acts as a multicopy suppressor of *sed5–1* (Banfield *et al.*, 1995); however, under the conditions used, this suppression was quite inefficient. In any case, Figure 4 shows that GFP-Sft2p rapidly dispersed into presumptive vesicles as the *sed5–1* strain was raised to the nonpermissive temperature. As with *sec18*, the effect was fully reversible. In this strain there was a noticeably higher-than-normal hazy background of fluorescence at the permissive temperature. This may reflect partial inactivation of this allele of Sed5p, even at low temperatures, resulting in some accumulation of vesicles.

A similar result was obtained with the temperature-sensitive allele *sft1–15* (Figure 4). Sft1p, which colocalizes with Sft2p (Banfield *et al.*, 1995; Figure 1*A*), is a putative vesicle SNARE that interacts with Sed5p and is essential for secretion, and we have previously proposed that it mediates the fusion of retrograde intra-Golgi vesicles with the early Golgi. The dispersal of GFP-Sft2p in *sft1–15* cells is consistent with this. The result is particularly striking, since upon prolonged incubation at the nonpermissive temperature *sft1* alleles accumulate relatively large membranous organelles (Banfield *et al.*, 1995). Our proposed role for Sft1p would predict that these are early-Golgi cisternae that are unable to receive retrograde vesicles, and this is borne out by the observation that Sft2p, a late marker, was not present in large structures.

To directly examine the fate of early cisternae, we also examined GFP-Sed5p in *sft1–15* cells and found that its distribution, unlike that of GFP-Sft2p, was punctate at both permissive and nonpermissive temperatures (Figure 5). Thus, as predicted, the morphology of the early-Golgi cisternae appears not to be directly affected by inactivation of Sft1p.

As an additional control, we examined the fate of GFP-Sft2p in a *sec14* mutant. As with *sft1–15*, *sec14* mutants rapidly block transport through the Golgi complex and cause the accumulation of abnormal Golgi membranes, often in stacks (Novick *et al.*, 1981). However, in contrast to the situation in *sft1* mutants, *sec14* cells are thought to be defective in budding from the late Golgi and thus might be expected to accumu-

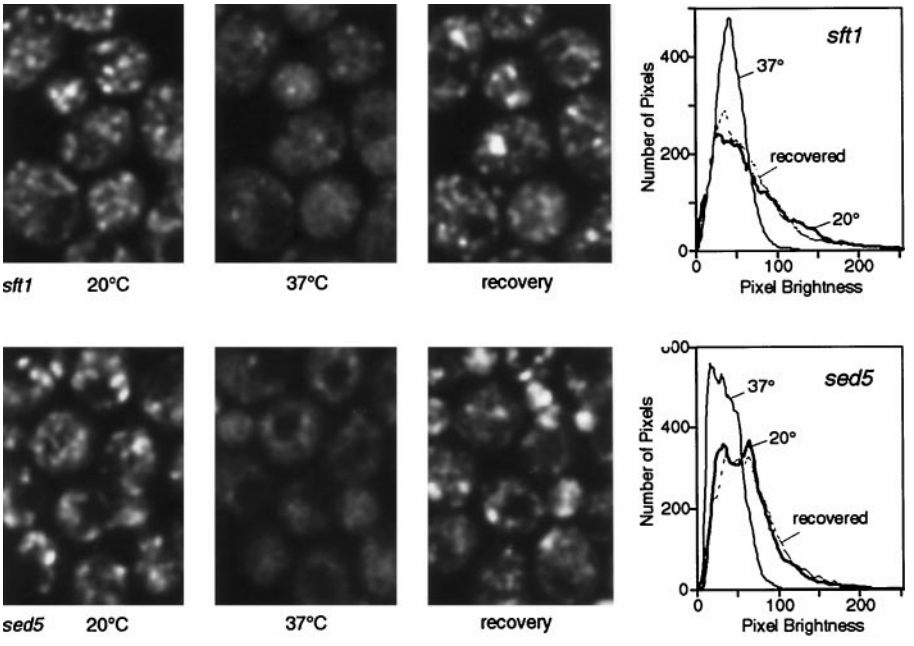

Figure 4. Dispersal of GFP-Sft2p in *sft1* and *sed5* mutants. Experiments were performed as in Figure 3. The dark areas in the cells at 37°C correspond to vacuoles. Note the loss and subsequent recovery of bright pixels revealed by the graphs. The slight residual punctate pattern in *sft1–15* cells may be due to incomplete inactivation of Sft1p; other alleles showed less of this but also had a partial phenotype at 20°C.

late late compartments (Kearns *et al.*, 1997). Figure 5 shows that GFP-Sft2p was found in somewhat larger structures than normal in a *sec14–3* strain, and the pattern did not change significantly after incubation for up to 40 min at the nonpermissive temperature. Thus, the effects of *sft1* and *sed5* on the distribution of GFP-Sft2p cannot be explained as mere side effects of any block to Golgi function.

Recycling of Sed5p

The cisternal maturation model predicts that early-Golgi cisternae are converted into late cisternae, and this means that they must lose Sed5p. The model also requires that new cisternae are formed from the ER, a process that could be explained if Sed5p cycles through the ER and is present in the vesicles that bud from it, and thus can mediate their fusion with each other to form Golgi cisternae (Pelham, 1998). To test this prediction, we examined whether it was possible to trap Sed5p in the ER using a mutant such as *sec12* that blocks vesicle budding from the ER, but not recycling to it. This strategy has been used previously to demonstrate recycling through the ER of other Golgi proteins such as Emp47p and Erd2p (Schröder *et al.*, 1995; Lewis and Pelham, 1996).

Figure 6A shows that the location of GFP-Sed5p changed in *sec12–4* cells. Within 30 min of a shift to the nonpermissive temperature, the punctate pattern was replaced by a typical ER distribution, with nuclear envelope and peripheral ER clearly visible (compare BiP staining in Figure 1A), whereas no such change occurred in SEC^+ cells (Figure 6B). A few bright dots were observed in the *sec12* cells after the shift and persisted even in longer incubations. These may not represent Golgi membranes, however; they were usually associated with the ER and may correspond to "BiP bodies," structures containing both ER markers and secretory proteins that appear when normal budding is blocked (Nishikawa *et al.*, 1994).

A complication of this experiment is that newly synthesized protein will also accumulate in the ER at the nonpermissive temperature. This can be prevented by inhibiting protein synthesis with cycloheximide, but we found that pretreatment of cells with cycloheximide for 20–30 min (necessary to allow preparation for imaging and temperature adjustment) prevented the loss of GFP-Sed5p from the Golgi. Since we have also observed effects on other Golgi proteins, such as an inhibition of retrograde transport of Emp47p, it seems likely that cycloheximide affects the normal dynamics of Golgi traffic under these conditions. A similar effect of cycloheximide has been observed in animal cells (Cole *et al.*, 1998).

As an alternative strategy, we used photobleaching to estimate the contribution of newly synthesized GFP-Sed5p to the ER-staining pattern. Preliminary experiments showed that fluorescence reappeared after bleaching over a period of 1–2 h, and that this recovery was prevented by cycloheximide. This indicates that the bleached GFP does not recover its fluorescence and also that the bleaching process neither inhibits subsequent protein synthesis nor (in more prolonged experiments) slows cell division. Figure 6C shows an experiment in which GFP-Sed5p was imaged in *sec12*

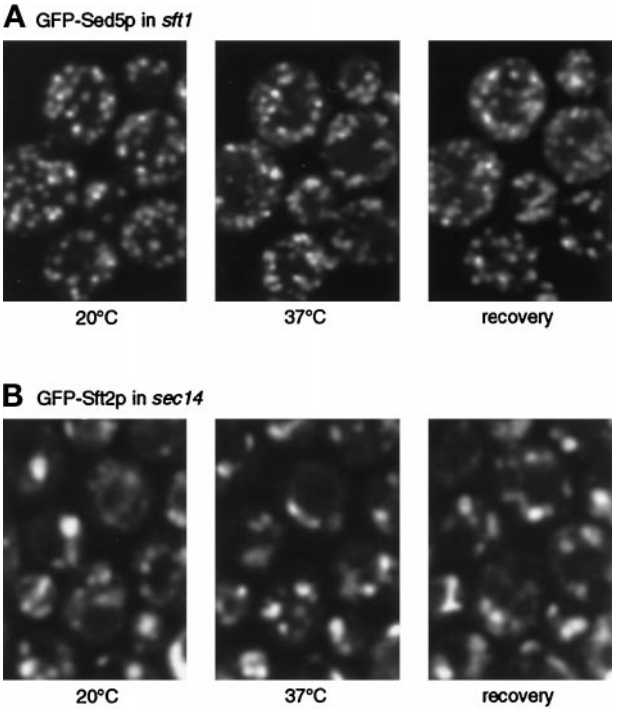

Figure 5. Specificity of the dispersal phenomenon. Experiments were performed as in Figures 3 and 4. (A) unlike GFP-Sft2p, GFP-Sed5p does not disperse in *sft1* cells. (B) GFP-Sft2p does not disperse in *sec14* cells. In this experiment the 37° image was taken 16 min after initiation of warming to ensure full onset of the secretory block; the pattern did not change during a further 20-min incubation at 37°C.

cells at low temperature, after which part of the image area was bleached and the cells were immediately warmed. The GFP-Sed5p was then imaged at intervals. Although dilution of the fluorescent protein into the relatively large area of ER membrane makes the images faint, it is clear that loss of the protein from Golgi membranes and its appearance in the ER occurs quite rapidly, between 5 and 15 min after the initiation of warming. In contrast, the appearance of GFP-Sed5p in the ER of bleached cells, which reflects new synthesis of the protein, occurred much more slowly. We conclude that pre-existing GFP-Sed5p moves to the ER in *sec12* cells and infer that Sed5p normally cycles through the ER. The rate of recycling appears comparable to that of Sft2p; it may be slightly underestimated by the experiment shown in Figure 6C because, to aid detection of Sed5p, we used a strain expressing twice as much GFP-Sed5p as endogenous Sed5p.

The loss of Sed5p from early Golgi compartments should have other measurable consequences. In particular, it should make early cisternae unable to receive Sft2p-containing vesicles from late cisternae, and a *sec12* strain should therefore show defects in GFP-Sft2p localization at the nonpermissive temperature. As shown in Figure 7, this was readily observable within 10 min of a temperature shift. Interestingly, the GFP-Sft2p appeared to accumulate in vesicles, as indicated by the characteristic hazy staining, rather than being delivered to the ER. The hazy pattern persisted during longer incubations at the nonpermissive temperature; only after very long times (2–3 h) did ER staining become visible, presumably due to the accumulation of newly synthesized protein (our unpublished results). Thus, although Sed5p moves to the ER in *sec12* cells, it does not appear to act as an efficient acceptor for retrograde vesicles in this location. The vesicles remained competent for fusion, because on return to the permissive temperature the punctate Golgi staining reappeared. Photobleaching of the cells before recovery greatly delayed the reappearance of Golgi staining, indicating that it was due to the delivery of pre-existing, rather than newly synthesized, GFP-Sft2p (our unpublished results). Indeed, the entire cycle of loss and recovery of the Golgi distribution of GFP-Sft2p could be completed within 25 min, a time too short to allow replenishment of the protein by synthesis.

Movement of Glycosyltransferases

Sed5p is a component of the transport machinery, and Sft2p might also be, although its precise function is unknown. It could thus be argued that these proteins are selectively recycled as part of their function. To determine whether more-typical Golgi residents behave in the same way, we examined the fate of two glycosyltransferases, Anp1p and Mnn1p. Immunofluorescence was used to detect them, because GFP chimeras containing these proteins did not give useful levels of Golgi fluorescence. Anp1p is a component of the elongating α1–6 mannosyltransferase and largely colocalizes with Sed5p (Jungmann and Munro, 1998; Figure 1A). We first established that we could detect recycling of an epitope-tagged version of Sed5p to the ER by immunofluorescence. Figure 8A shows that after a 15-min incubation of *sec12* cells at the nonpermissive temperature, the tagged Sed5p showed an ER distribution comparable to that of GFP-Sed5p, although slightly more punctate. Under these conditions the typical Golgi staining observed for Anp1p disappeared, being replaced by a more even distribution, with dark areas corresponding to nuclei and vacuoles (Figure 8B). Detailed images of a single confocal plane revealed a fine dotted appearance. Based on the optical properties of the microscope (very small light sources give an image with an apparent width of about 250 nm), we estimate that 40 or more vesicular structures per cell section would be sufficient to generate the observed pattern. No staining of the nuclear envelope or other ER membranes could be detected. In

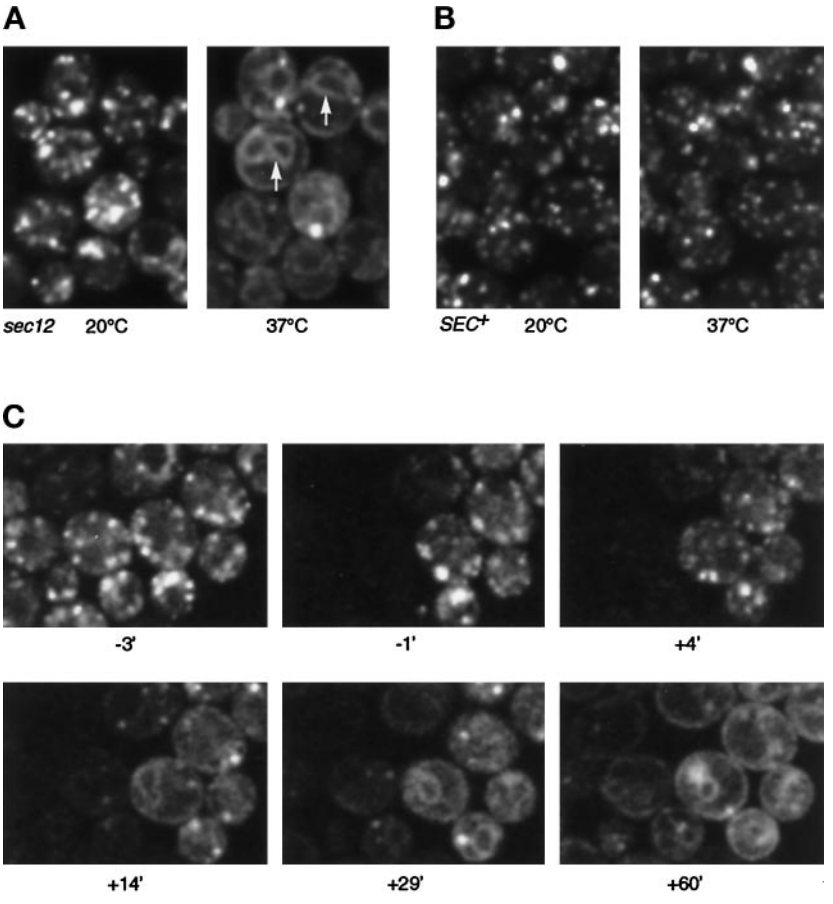

Figure 6. GFP-Sed5p moves to the ER in *sec12* cells. (A) Single optical sections showing GFP-Sed5p in *sec12* cells at 20°C and at 37°C (30 min after initiation of warming). Arrows indicate nuclear envelope fluorescence (compare BiP staining in Figure 1). (B) Control showing GFP-Sed5p in *SEC*$^+$ cells. (C) Time course of movement of GFP-Sed5p in *sec12* cells. Images (single optical sections) were taken at the times indicated (min), zero being the point at which heating was initiated. Just before the −1 time point, the left half of the field was photobleached. Note that the loss of punctate fluorescence and the emergence of the ER pattern in the unbleached cells occurred more rapidly than the reappearance of fluorescence in the bleached cells.

contrast, Anp1p staining remained punctate in *sec14* and *SEC*$^+$ cells at 37°C (Figure 8).

To confirm the different behavior of Sed5p and Anp1p in *sec12* cells, we prepared membrane fractions sedimenting at 13,000 × *g* (p13) and 100,000 × *g* (p100) from cells incubated at 37°C. In such preparations ER is found almost exclusively in the p13 fraction, as shown by immunoblotting with antibodies to Sec61p, whereas Golgi markers distribute between the p13 and the p100 fractions. Emp47p, a Golgi protein previously shown to recycle through the ER (Schröder *et al.*, 1995; Lewis and Pelham, 1996), was depleted from the p100 fraction in *sec12* cells (Figure 9). Sed5p behaved like Emp47p, as expected from the fluorescence results. In contrast, slightly more of the Anp1p was found in the p100 fraction in *sec12* cells than in the control strain. The late Golgi marker GFP-Sft2p also remained in the p100 fraction in *sec12* cells (Figure 9), confirming that it does not follow Sed5p to the ER.

We conclude that, unlike Sed5p, the bulk of Anp1p does not recycle through the ER. However, it does not remain stationary, but enters small vesicle-like structures that, in *sec12* cells, are unable to fuse. If these correspond to the structures that GFP-Sft2p enters, then Anp1p should also be trapped in them in *sft1* cells incubated at 37°C. Under these conditions there was indeed a signif-

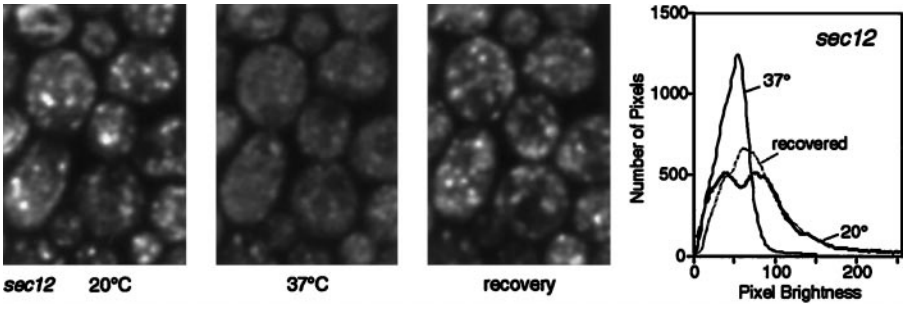

Figure 7. GFP-Sft2p dispersal in *sec12* cells. The experiment was performed as in Figures 3 and 4.

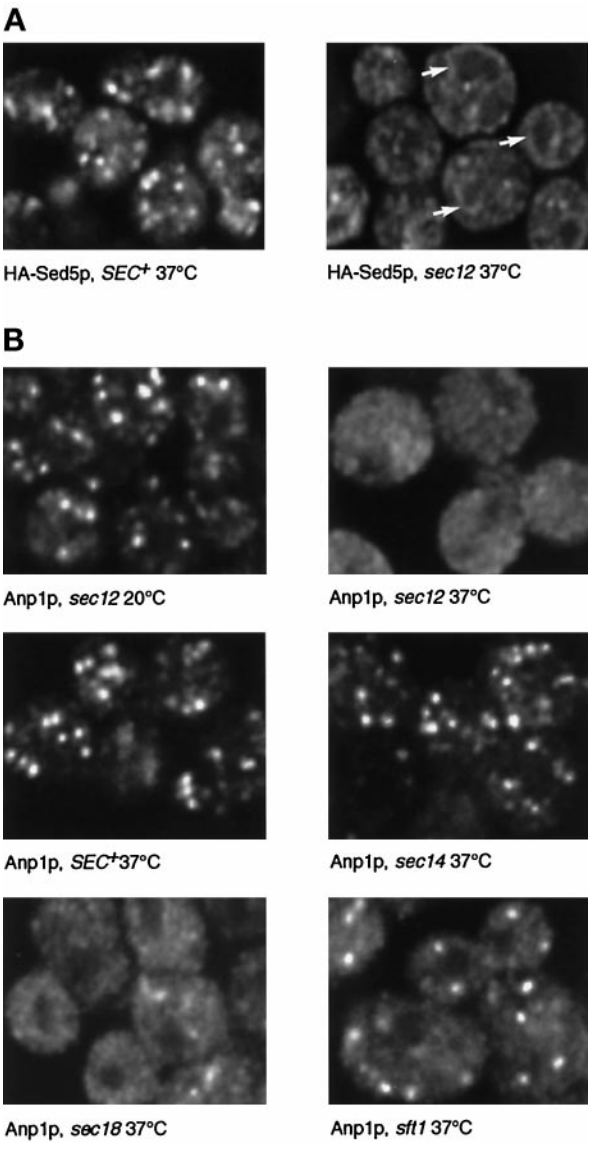

Figure 8. Dispersal of the early-Golgi marker Anp1p. (A) Cells of the indicated genotypes expressing epitope-tagged Sed5p were shifted from 20°C to 37°C for 15 min, fixed, and stained with appropriate antibodies to detect the tagged Sed5p. Arrows indicate nuclear envelope (i.e., ER) staining. (B) Cells of the indicated genotypes were incubated at 20°C or shifted to 37°C for 15 min, fixed, and stained with anti-Anp1p antibodies. Single confocal sections are shown in each case.

icant dispersal of the Anp1p (Figure 8B). However, some punctate staining remained, and this persisted even when the cells were held at the nonpermissive temperature for 60 min. More complete dispersal was observed with *sec18* cells (Figure 8B) and *sed5* cells (our unpublished observations). It is not clear whether this difference is due to residual activity of the *sft1–15* allele, or to Anp1p entering two kinds of vesicle, only one of which requires Sft1p for fusion.

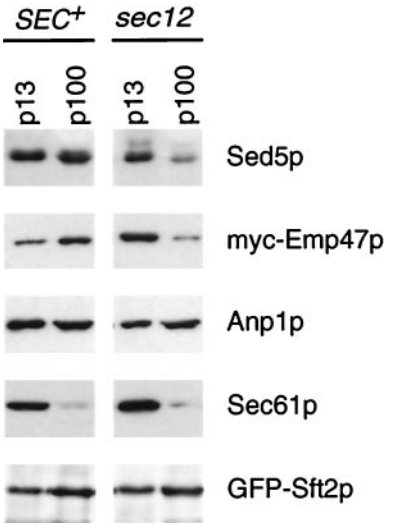

Figure 9. Subcellular fractionation of Golgi proteins in *sec12* cells. SEC^+ and *sec12* strains expressing either GFP-Sft2p or a myc-tagged version of Emp47p (Lewis and Pelham, 1996) were incubated at 37°C for 90 min, and medium-speed (p13) and high-speed (p100) pellet fractions were prepared. These were immunoblotted with appropriate antibodies as indicated.

Mnn1p adds the terminal α1–3-linked mannose residues to glycoproteins and is considered a typical late-Golgi enzyme (Yip *et al.*, 1994). Using an epitope-tagged version of this protein, we observed punctate staining in SEC^+ and *sec14* cells at both 20°C and 37°C. However, within 15 min of warming *sed5* or *sft1* mutants, the staining pattern changed to a finely punctate distribution, similar to the pattern of GFP-Sft2p under these conditions, or of Anp1p in *sec12* cells (Figure 10). Thus, the behavior of this enzyme is very similar to that of Sft2p.

Vesiculation of Golgi Membranes

All four of the resident Golgi proteins examined rapidly entered dispersed structures under conditions in which vesicle fusion was inhibited. Since most Golgi proteins are residents, this suggests that a substantial fraction of the Golgi membrane might vesiculate, and we sought evidence for this by electron microscopy. Yeast Golgi membranes have been identified by immuno-EM, and their appearance in thin sections of permanganate-fixed cells has been described. They are typically visible as short membrane profiles up to 400 nm long, often curved, and sometimes aligned in pairs or, rarely, threes (Preuss *et al.*, 1992; Figure 11). Significantly, such profiles are absent from *sec12*, *sec17*, or *sec18* cells incubated for 1 h at the nonpermissive temperature (see Kaiser and Schekman, 1990, for examples), suggesting that Golgi cisternae are indeed unstable under these conditions.

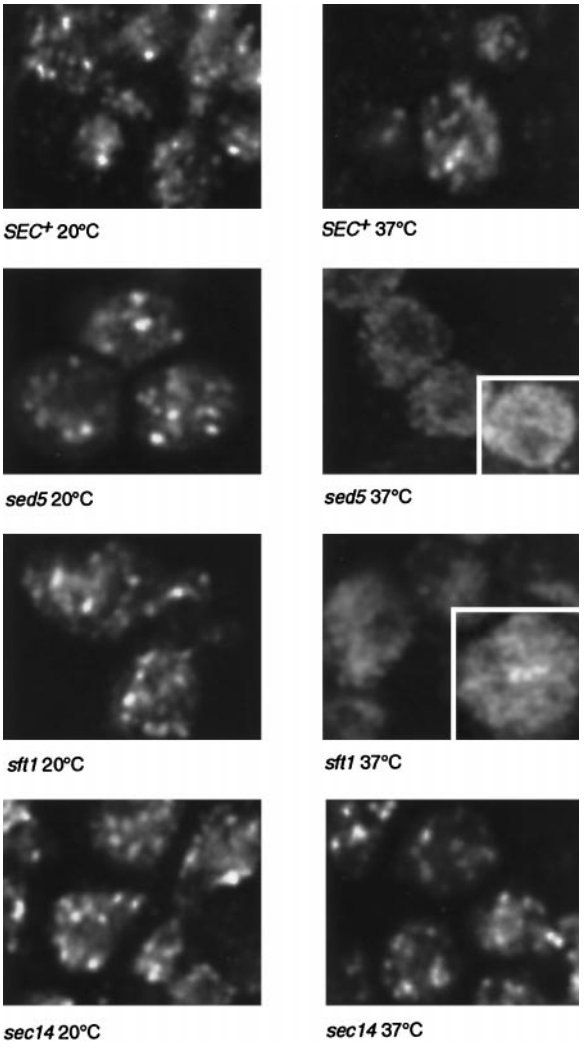

Figure 10. Dispersal of the late-Golgi marker Mnn1p. Cells expressing epitope-tagged Mnn1p were incubated at 20°C or for 15 min at 37°C as indicated, fixed, and stained with tag-specific antibodies as in Figure 8. Single confocal sections are shown; the outlined regions have the brightness increased to show the appearance of the dispersed staining more clearly.

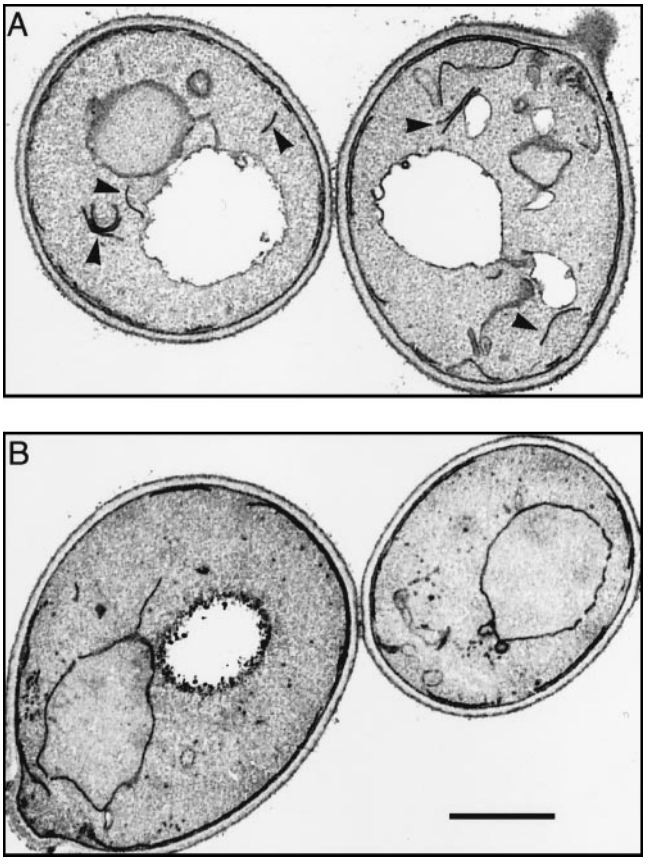

Figure 11. Electron microscopy of *sec18* cells. Panel A shows cells incubated at 17°C (permissive temperature). Arrows indicate membrane profiles typical of the Golgi apparatus. Panel B shows cells fixed 10 min after a shift to 37°C. Putative Golgi profiles are virtually absent, and many small vesicles have accumulated. Bar, 1 μm.

The *sec18–1* mutation acts rapidly after temperature shift, and since it blocks essentially all fusion events, it should provide a measure of the speed and extent of Golgi vesiculation. Figure 11 shows some typical Golgi profiles from *sec18* cells incubated at permissive temperature (17°C). For the purposes of quantitation, we included all linear membrane segments that were neither juxtaposed to the plasma membrane nor obviously connected to the nuclear envelope or peripheral ER. The average content of such membranes was 0.2 μm per μm^2 of section. This procedure may overestimate the Golgi content, since some ER segments or other organelles may also be included. In cells fixed 10 min after a shift to 37°C, aligned cisternae were very rare, and the content of possible Golgi membranes had dropped by 75%, to 0.05 $\mu m/\mu m^2$. This was more than compensated for by the accumulation of small (~50-nm) vesicles, numbering about 60 per μm^3, which were presumably derived from both ER and Golgi membranes (Kaiser and Schekman, 1990; Lewis and Pelham, 1996). Incubation of the cells for a further 50 min at 37°C did not substantially change this pattern.

Since *sec18* cells lose typical Golgi profiles and accumulate only small vesicles and fragments, we infer that a substantial proportion of Golgi membranes can be converted into vesicles within 10 min. This correlates well with the immunofluorescence studies. In particular, assuming that in the steady state about half the Golgi cisternae contain any one enzyme, and that the enzymes are not substantially concentrated during vesiculation, one would expect an enzyme to be present in about 60 vesicles in a 0.3-μm-thick optical section.

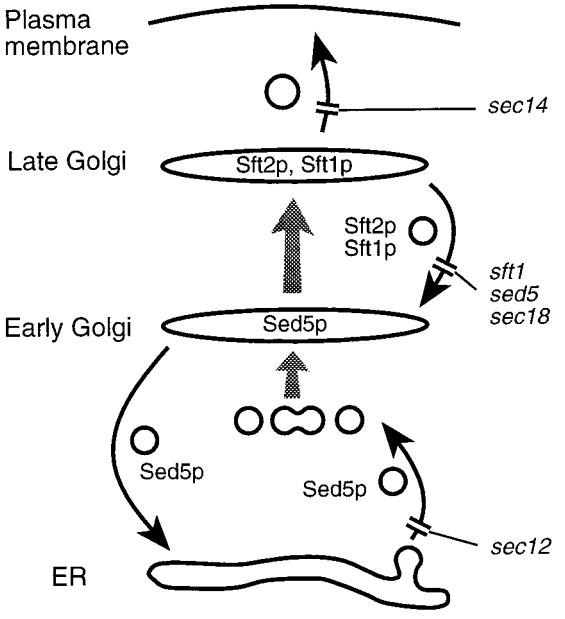

Figure 12. Model and summary of results. A model of membrane traffic in the yeast Golgi, based on previous results, is depicted. Curved arrows indicate vesicular transport steps, and the steady-state locations of Sft2p, Sft1p, and Sed5p are shown. The sites at which the various mutations act are also shown. Note that only the molecules and effects relevant to the data in this paper are indicated, and that *sec18*, for example, will block other steps also. Gray arrows represent maturation of cisternae, but the data in this paper do not exclude the possibility of vesicular transport from early to late Golgi. The model accounts for the observations that Sft2p (and Mnn1p, which has a similar location) disperses in small structures (vesicles) in *sft1*, *sed5*, *sec18*, and *sec12*, but not in *sec14*, and that Sed5p moves to the ER in *sec12* but remains in Golgi cisternae in *sft1*. Anp1p, although largely colocalizing with Sed5p, recycles within the Golgi rather than returning to the ER.

DISCUSSION

In this paper we have shown that it is possible to observe Golgi membrane dynamics in living yeast cells using GFP chimeras and have characterized two such chimeras, GFP-Sft2p and GFP-Sed5p, in detail. In addition to the distribution and movement of Golgi membranes in wild-type cells, we have studied the changes that occur when various components of the Golgi trafficking machinery are inactivated by temperature-sensitive mutations. Figure 12 summarizes our results and places them in a simple model. Sft2p and Sft1p seem normally to be resident in punctate structures that correspond to later Golgi cisternae than those marked by Sed5p. However, GFP-Sft2p can enter much smaller structures, presumably vesicular in nature. Fusion of these presumptive vesicles is blocked rapidly and reversibly by mutations in *sec18*, *sft1*, and *sed5*. Given the good genetic and biochemical evidence that Sft1p contacts Sed5p directly (Banfield *et al.*, 1995; Søgaard *et al.*, 1994; Holthuis *et al.*, 1998), the simplest explanation for this is that the vesicles normally fuse with early Golgi cisternae containing Sed5p, and that Sft1p acts as a v-SNARE for this step.

Sed5p, in turn, can recycle to the ER, where it becomes trapped when a *sec12* mutant is incubated at a nonpermissive temperature. Probably because of this, Sft2p-containing vesicles are unable to fuse to Golgi membranes under these conditions, but they are not redirected to the ER even though Sed5p accumulates there. This demonstrates clearly that retrograde transport of Sft2p is quite distinct from the retrieval of ER proteins and also shows that the destination of these vesicles is not defined simply by the presence of Sed5p.

In addition to the GFP chimeras, we also examined two Golgi mannosyltransferases, Anp1p and Mnn1p. Mnn1p, a late Golgi marker, behaved like GFP-Sft2p, implying that it cycles through earlier cisternae. Anp1p was found largely in the same structures as Sed5p and, like Sed5p, it left these structures in a *sec12* mutant. However, it did not move to the ER but instead appeared to reach later cisternae and then enter retrograde intra-Golgi vesicles. This behavior is reminiscent of that of another early-Golgi marker Och1p, which also fails to move to the ER in a *sec12* mutant, but seems to cycle through a later compartment containing the protease Kex2p (Schröder *et al.*, 1995; Harris and Waters, 1996). Hence, both early- and late-Golgi markers cycle within the Golgi complex. This does not necessarily mean that they follow precisely the same route. They may enter retrograde vesicles with different efficiencies or at different points, and it is also possible that they are delivered to different subsets of Sed5p-containing cisternae. The presence of multiple Golgi SNAREs offers considerable scope for complexity.

The apparent ease with which Golgi markers enter vesicles is also reflected in morphological changes. Examination of published electron micrographs shows that the characteristic Golgi structures described by Preuss *et al.* (1992) disappear when *sec12* or *sec17* cells are incubated at a nonpermissive temperature (e.g., Kaiser and Schekman, 1990), but this has not previously been commented on. We have confirmed the result with *sec18* cells and conclude that much of the Golgi membrane can be converted into vesicles or small fragments.

Interestingly, not all blocks to ER-Golgi traffic cause complete fragmentation of Golgi membranes. Residual structures remain in *sec20* and *ufe1* mutants (e.g., Lewis and Pelham, 1996), and we have confirmed that GFP-Sft2p persists in punctate structures in *sec20* cells at 37°C (our unpublished observations). These mutants block forward transport indirectly, by inhibiting retrograde traffic to the ER, and thus do not trap Sed5p in the ER. Their effects are consistent with the idea that it is the loss of recycling fusion components from the

early Golgi that causes late Golgi markers to accumulate in vesicles.

The speed of vesiculation is striking. The changes we observed by electron microscopy, immunofluorescence, or direct visualization of GFP chimeras all occurred within 10 min of shifting mutant cells to 37°C. For comparison, proteins such as invertase or α factor pass from the ER to the cell surface in ~5 min under optimal conditions (Novick *et al.*, 1981); at 37°C, transport is slower and secretion of α factor is still incomplete after 10 min (Graham and Emr, 1991). Hence, entry of resident Golgi proteins into vesicles occurs on the same timescale as secretion.

How do these observations fit with current views of intra-Golgi traffic? Our favored model involves cisternal maturation, the conversion of early to late cisternae by means of retrograde vesicular traffic of Golgi resident proteins (Pelham, 1998). This makes a strong testable prediction: that all resident Golgi proteins, including target SNAREs such as Sed5p, should enter retrograde vesicles within the time that it takes a secretory protein to transit through the Golgi complex. Our data support this prediction, and hence the model remains viable. In contrast, models in which cisternae have a stable existence, with secretory proteins passing between them in vesicles, make no clear prediction about the recycling of resident proteins. However, they would seem best served by the residents remaining relatively stationary, and thus fit less well with the data. Whatever model is assumed, it seems clear that Golgi membranes are highly dynamic; cisternae either have a very limited lifespan or are maintained by a delicate balance of rapid budding and fusion.

One implication of this study is that at least two distinct types of retrograde vesicle must originate in the Golgi, bearing different SNAREs and destined for Sed5p-containing cisternae and the ER, respectively. There is good evidence that traffic to the ER is mediated by COPI coats (Letourneur *et al.*, 1994; Lewis and Pelham, 1996), and since there are no other candidates, it is likely that retrograde intra-Golgi traffic is also mediated by coat protein I (COPI) coats. However, this has proved difficult to demonstrate in yeast, since the available COPI mutants do not block passage through the Golgi and may not prevent vesicle formation (Letourneur *et al.*, 1994; Lewis and Pelham, 1996). Electron microscopic studies in pancreatic cells do suggest heterogeneity in Golgi-derived COPI-coated vesicles (Orci *et al.*, 1997, 1998), but the relationship of the observed vesicle populations to the predicted retrograde ones, or to possible anterograde carriers, is not easy to determine.

If COPI coats are used for both types of retrograde vesicle, how are the contents distinguished? Why do recycling Golgi proteins, such as Sft2p and Anp1p, not go with Sed5p to the ER? A possible explanation is that the sorting of such proteins is determined in part by interactions between their transmembrane segments and membrane lipids (reviewed by Munro, 1998), and that differences in the lipid composition of early and late cisternae regulate their entry into COPI vesicles.

Despite the obvious morphological differences, the basic features of Golgi traffic are likely to be similar in animal cells and yeast, and recent studies support this. It has been shown that the mammalian homologue of Sed5p, syntaxin 5, recycles through the ER (Rowe *et al.*, 1998), and that structures related to the cis-Golgi network can be formed de novo by vesicles budding from the ER and undergoing homotypic fusion (Presley *et al.*, 1997; Scales *et al.*, 1997). Moreover, Golgi-specific modification of vesicular stomatitis virus glycoprotein in an ER–Golgi transport assay requires both ER-derived syntaxin 5 and the Golgi v-SNARE GOS28, but does not require syntaxin 5 on the Golgi membranes (Nagahama *et al.*, 1996; Subramaniam *et al.*, 1996; Rowe *et al.*, 1998). Finally, it has been reported that Golgi-derived vesicles preferentially incorporate resident Golgi enzymes rather than anterograde cargo molecules (Love *et al.*, 1998). All these findings are consistent with the idea that ER-derived transport vesicles fuse with each other to form early-Golgi cisternae, to which enzymes are delivered by retrograde intra-Golgi transport (Figure 12; Pelham, 1998).

ACKNOWLEDGMENTS

We are grateful to Mike Lewis and Douglas Kershaw for preparation of the electron microscopic sections of *sec18* cells. We also thank our numerous colleagues, in particular Mike Lewis, Julian Rayner, Sean Munro, Jim Haseloff, and Brad Amos, for advice, reagents, and helpful discussions, and Ben Nichols and Joost Holthuis for comments on the manuscript.

REFERENCES

Banfield, D.K., Lewis, M.J., and Pelham, H.R.B. (1995). A SNARE-like protein required for traffic through the Golgi complex. Nature *375*, 806–809.

Cole, N.B., Ellenberg, J., Song, J., DiEuliis, D., and Lippincott-Schwartz, J. (1998). Retrograde transport of Golgi-localized proteins to the ER. J. Cell Biol. *140*, 1–15.

Cormack, B.P., Valdivia, R.H., and Falkow, S. (1996). FACS-optimized mutants of the green fluorescent protein (GFP). Gene *173*, 33–38.

Farquhar, M.G. (1985). Progress in unraveling pathways of Golgi traffic. Annu. Rev. Cell Biol. *1*, 447–488.

Fischer von Mollard, G., Nothwehr, S.F., and Stevens, T. (1997). The yeast v-SNARE Vti1p mediates two vesicle transport pathways through interactions with the t-SNAREs Sed5p and Pep12p. J. Cell Biol. *137*, 1511–1524.

Graham, T.R., and Emr, S.D. (1991). Compartmental organisation of Golgi-specific protein modification and vacuolar protein sorting events defined in a yeast *sec18* (NSF) mutant. J. Cell Biol. *114*, 207–218.

Hardwick, K.G., and Pelham, H.R.B. (1992). SED5 encodes a 39kD integral membrane protein required for vesicular transport between the ER and the Golgi complex. J. Cell Biol. *119*, 513–521.

Harris, S.L., and Waters, G.M. (1996). Localisation of a yeast early Golgi mannosyltransferase, Och1p, involves retrograde transport. J. Cell Biol. *132*, 985–998.

Heim, R., and Tsien, R.Y. (1996). Engineering green fluorescent protein for improved brightness, longer wavelengths and fluorescence resonance energy transfer. Curr. Biol. *6*, 178–182.

Holthuis, J.C.M., Nichols, B.J., Dhruvakumar, S., and Pelham, H.R.B. (1998). Two syntaxin homologues in the TGN/endosomal system of yeast. EMBO J. *17*, 113–126.

Jungmann, J., and Munro, S. (1998). Multi-protein complexes in the cis Golgi of *Saccharomyces cerevisiae* with alpha 1,6-mannosyltransferase activity. EMBO J. *17*, 423–434.

Kaiser, C.A., and Schekman, R. (1990). Distinct sets of SEC genes govern transport vesicle formation and fusion early in the secretory pathway. Cell *61*, 723–733.

Kearns, B.G., McGee, T.P., Mayinger, P., Gedvilaite, A., Phillips, S.E., Kagiwada, S., and Bankaitis, V.A. (1997). Essential role for diacylglycerol in protein transport from the yeast Golgi complex. Nature *387*, 101–105.

Kilmartin, J.V., and Adams, A.E. (1984). Structural rearrangements of tubulin and actin during the cell cycle of the yeast *Saccharomyces*. J. Cell Biol. *98*, 922–933.

Letourneur, F., Gaynor, E.C., Hennecke, S., Démollière, C., Duden, R., Emr, S., Riezman, H., and Cosson, P. (1994). Coatomer is essential for retrieval of dilysine-tagged proteins to the endoplasmic reticulum. Cell *79*, 1199–1207.

Lewis, M.J., and Pelham, H.R.B. (1996). SNARE-mediated retrograde transport from the Golgi complex to the ER. Cell *85*, 205–215.

Love, H.D., Lin, C., Short, C.S., and Ostermann, J. (1998). Isolation of functional Golgi derived vesicles with a possible role in retrograde transport. J. Cell Biol. *140*, 541–551.

Lupashin, V.V., Pokrovskaya, I.D., McNew, J.A., and Waters, M.G. (1997). Characterization of a novel yeast SNARE protein implicated in Golgi retrograde traffic. Mol. Biol. Cell *8*, 2659–2676.

McNew, J.A., Søgaard, M., Lampen, N.M., Machida, S., Ruby Ye, R., Lacomis, L., Tempst, P., Rothman, J.E., and Söllner, T. (1997). Ykt6p, a prenylated SNARE essential for endoplasmic reticulum–Golgi transport. J. Biol. Chem. *272*, 17776–17783.

Mironov, A.A., Weidman, P., and Luini, A. (1997). Variations on the intracellular transport theme: maturing cisternae and trafficking tubules. J. Cell Biol. *138*, 481–484.

Munro, S. (1998). Localisation of proteins to the Golgi apparatus. Trends Cell Biol. *8*, 11–15.

Nagahama, M., Orci, L., Ravazzola, M., Amherdt, M., Lacomis, L., Tempst, P., Rothman, J.E., and Söllner, T.H. (1996). A v-SNARE implicated in intra-Golgi transport. J. Cell Biol. *133*, 507–516.

Napier, R.M., Fowke, L.C., Hawes, C., Lewis, M., and Pelham, H.R.B. (1992). Immunological evidence that plants use both HDEL and KDEL for targeting proteins to the endoplasmic reticulum. J. Cell Sci. *102*, 261–271.

Nichols, B.J., Ungermann, C., Pelham, H.R.B., Wickner, W.T., and Haas, A. (1997). Homotypic vacuolar fusion mediated by t- and v-SNAREs. Nature *387*, 199–202.

Nishikawa, S., Hirata, A., and Nakano, A. (1994). Inhibition of endoplasmic reticulum (ER)-to-Golgi transport induces relocalization of binding protein (BiP) within the ER to form the BiP bodies. Mol. Biol. Cell *5*, 1129–1143.

Novick, P., Ferro, S., and Schekman, R. (1981). Order of events in the yeast secretory pathway. Cell *25*, 461–469.

Orci, L., Perrelet, A., and Rothman, J.E. (1998). Vesicles on strings: morphological evidence for processive transport within the Golgi stack. Proc. Natl. Acad. Sci. USA *95*, 2279–2283.

Orci, L., Stamnes, M., Ravazzola, M., Amherdt, M., Perrelet, A., Sollner, T.H., and Rothman, J.E. (1997). Bidirectional transport by distinct populations of COPI-coated vesicles. Cell *90*, 335–349.

Palade, G. (1975). Intracellular aspects of the process of protein synthesis. Science *189*, 347–358.

Pelham, H.R.B. (1998). Getting through the Golgi complex. Trends Cell Biol. *8*, 45–49.

Presley, J.F., Cole, N.B., Schroer, T.A. Hirschberg, K., Zaal, K.J.M., and Lippincott-Schwartz, J. (1997). ER to Golgi transport visualised in living cells. Nature *389*, 81–85.

Preuss, D., Mulholland, J., Franzusoff, A., Segev, N., and Botstein, D. (1992). Characterization of the *Saccharomyces* Golgi complex through the cell cycle by immunoelectron microscopy. Mol. Biol. Cell *3*, 789–803.

Rothman, J.E. (1994). Mechanisms of intracellular protein transport. Nature *372*, 55–63.

Rowe, T., Dascher, C., Bannykh, S., Plutner, H., and Balch, W.E. (1998). Role of vesicle-associated syntaxin 5 in the assembly of pre-Golgi intermediates. Science *279*, 696–700.

Scales, S.J., Pepperkok, R., and Kreis, T.E. (1997). Visualisation of ER-to-Golgi transport in living cells reveals a sequential mode of action for COPII and COPI. Cell *90*, 1137–1148.

Schekman, R., and Mellman, I. (1997). Do COPs go both ways? Cell *90*, 197–200.

Schekman, R., and Orci, L. (1996). Coat proteins and vesicle budding. Science *271*, 1526–1533.

Schnepf, E. (1993). Golgi-apparatus and slime secretion in plants—the early implications and recent models of membrane traffic. Protoplasma *172*, 3–11.

Schröder, S., Schimmöller, F., Singer-Krüger, B., and Riezman, H. (1995). The Golgi localisation of yeast Emp47p depends on its dilysine motif but is not affected by the *ret1–1* mutation in α-COP. J. Cell Biol. *131*, 895–912.

Sikorski, R.S., and Hieter, P. (1989). A system of shuttle vectors and yeast host strains designed for efficient manipulation of DNA in *Saccharomyces cerevisiae*. Genetics *122*, 19–27.

Søgaard, M., Tani, K., Ye, R.R., Geromanos, S., Tempst, P., Kirchhausen, T., Rothman, J.E., and Söllner, T. (1994). A Rab protein is required for the assembly of SNARE complexes in the docking of transport vesicles. Cell *78*, 937–948.

Subramaniam, V.N., Peter, F., Philp, R., Wong, S.H., and Hong, W. (1996). GS28, a 28-kilodalton SNARE that participates in ER-Golgi transport. Science *272*, 1161–1163.

Yip, C.L., Welch, S.K., Klebl, F., Gilbert, T., Seidel, P., Grant, F.J., O'Hara, P.J., and MacKay, V.L. (1994). Cloning and analysis of the *Saccharomyces cerevisiae* MNN9 and MNN1 genes required for complex glycosylation of secreted proteins. Proc. Natl. Acad. Sci. USA *91*, 2723–2727.